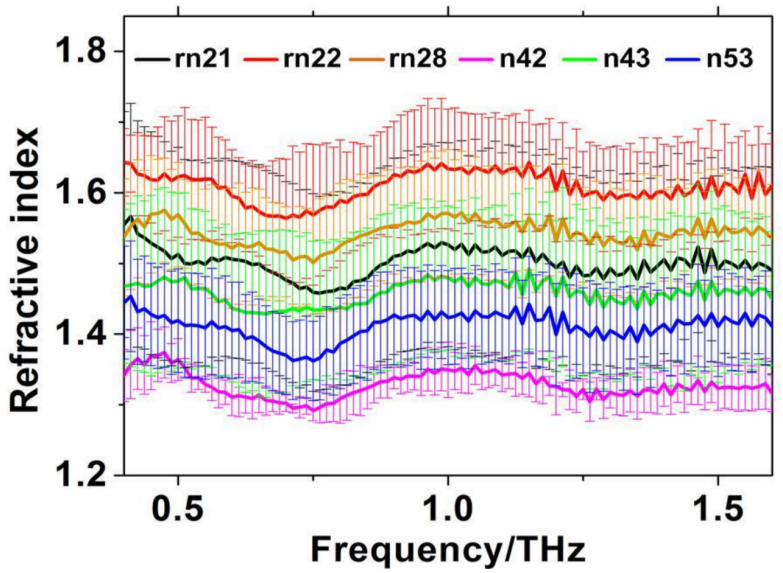

Figure 3. Refractive index of the proteins rn21, rn22, rn28, n42, n43 and n53 for samples with a concentration of 2.0 µg/µL and a quantity of 8 µg. Reprinted from Ref. [174].

The refractive index vs. frequencies in the THz range of these six different species of proteins are different and well-separated, allowing to distinguish each protein. Although the error bars overlap, the curve trend points out that the protein with a higher molecular mass has a stronger refraction capacity, namely a greater refractive index at every frequency. Authors have investigated the ability of THz imaging to differentiate and quantify the content of different kinds of specific proteins. The intensity or the level of shade of the image is directly related to the number of proteins participating in the absorption, see Figure 4. For this purpose, a nitrocellulose blotting membrane (NC) was dropped with liquid solutions of the six proteins, formulated inside the five solutions with corresponding concentrations of 2 µg/µL, 1 µg/µL, 0.5 µg/µL, 0.25 µg/µL and 0.125 µg/µL, dissolved in solution of 1 × PBS at pH 7.2. Observing Figure 4b, a variation of the average color-scale of proteins rn21, rn22 and n43 was evident; firstly, it increases at 0.5 µg, and then it decreases at 1 µg, 2 µg, 4 µg and 8 µg as a function of protein quantity (except for the 8 µg of Protein n43). At variance, the average color scales of proteins rn28 and n42 exhibit the opposite trend (see Figure 4b). For the six kinds of proteins with the same amount, the intensity of gray levels behaves similarly to the refractive index absorption. The THz experimental results of Han et al. match exactly the results of the dot blot (see Figure 4a) method. Besides, the application of THz spectroscopy does not merely distinguish the different proteins, it precisely acquires the protein quantity distribution, but it is able to reduce the time procedure compared to conventional immunoassays in the label-free and non-destructive mode.

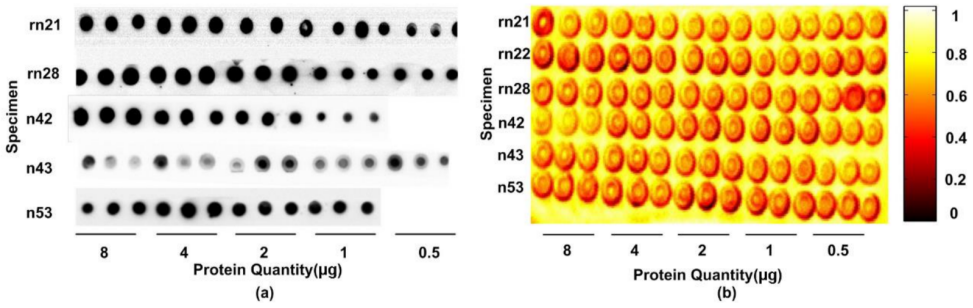

Figure 4. The imaging of the membrane: (**a**) the dot blot result, (**b**) the pseudo-color image of gray image formatted by the relative THz energy integration of transmission spectrum pixel by pixel. Reprinted from Ref.[174].

The structural flexibility of the protein allows to skillfully change its conformation without modifying the function it has to perform [175]. The frequency dependence of the density of the vibrational modes in the biological temperature range can quantify flexibility [163]. One example involves the transfer of cytochrome c (CytC) protein electrons. The CytC constituent amino acids have a covalently linked heme group with two oxidation states, ferri-and ferro-CytC. Ferri-CytC is less thermally stable than ferro-CytC and has also a higher hydrogen exchange and proteolytic digestion rate [169]. The THz spectroscopy was revealed as a powerful investigation tool because the collective vibrational modes fall into the THz domain, ranging from 0.03 to 6 THz (1–200 cm^{-1}) [176]. Chen and co-workers [175] examined the complex THz dielectric response of CytC films in the two oxidation states and found that absorption and refractive indexes tend to increase with the degree of oxidation. A sharp increase in the density of the vibrational modes and/or the dipole coupling in the interval is observed in the range 0.15–2.4 THz (5–80 cm^{-1}).

The influence of various physical and/or chemical factors [177–182] can induce protein denaturation with a relative change of the internal structure and properties of protein molecules. The structural change induced in the protein consequently alters its functionality, a delicate aspect in food processing, protein purification, nutrition, biomedicine and the food industry. Several examples underlined the advantage of THz technology in the study of protein denaturation and conformational changes. Studies with native sperm-whale myoglobin indicated that loss of secondary and tertiary structures influences the far-IR spectra as spectral changes in the region between 11.1 and 15.6 THz (370–520 cm^{-1}) along with broader changes around 6.0 THz (200 cm^{-1}) [183]. Firstly, the denaturation of the PsbO protein [184] and two photosynthesis chlorophyll proteins CP43 and CP47 [185–187] were examined though THz-TDS. Recently, a consistent, strong increase in the <3 THz (100 cm^{-1}) absorbance was shown in the measurements of non-native hen egg white lysozyme (HEWL) [188] and human serum albumin (HSA) [189]. Yoneyama et al. [162], using THz spectroscopy, measured the thermal denaturation of BSA protein held in a membrane device, observing a higher THz transmittance of the thermal denatured BSA sample compared to that of the native-conformation sample. Temperature-dependent THz analysis was also led by George et al. [190] on frozen-solution-phase samples of hen HEWL and CytC proteins, in order to study temperature-dependent conformation of proteins. The estimation of the imaginary part of the dielectric function as a function of T and fitting with Arrhenius model activation energies explained the behavior of HEWL being free, bonded to 3NAG and denatured; CytC was oxidized, reduced and denatured. The thermal denaturation of HSA in an aqueous buffer solution revealed changes in the absorption coefficient and refractive index as a function of the temperature [189].

Many of these experiments proved the feasibility of both protein and denaturation detection, but on the other hand they drew attention to some problems such as low signal-to-noise ratio and poor sensitivity, especially in the liquid environment because of water absorption. To overcome these limitations, different approaches can be adopted to enhance the THz response of biological samples based on graphene [191], on microfluidic chips [192,193], novel materials such as meta- and nano-materials [109,194–196], on gold nanoparticles [197] and on nanoantennas [198].

A promising further step forward in development of THz technology was given recently by Zhang's group [199]. They utilized the reflective THz time-domain polarization spectroscopy (THz-TDPS) method for protein sensing in the liquid environment in the spectral region 0.1–2.5 THz (3.33–83.3 cm^{-1}). The system, reported in Figure 5a,b, allows to obtain a polarization sensing, measuring the reflective polarization spectra for a liquid-phase sample. To this aim, a traditional transmission THz-TDS [97,98] was modified, adding a reflection module (Figure 5b) to the bottom of the 3D printing sample cell and two rotatable THz polarizers at the emitting end and detection ports of the spectroscopic system (Figure 5a). The advantage is to measure the states of signals without the strong THz water absorption in reflection mode. In addition, authors used a flexible twisted dual-layer metasurface structure with geometric chirality (Figure 5c–e), as a sensor, to enhance the

polarization response of three protein samples: BSA, whey protein (WP) and ovalbumin (OVA).

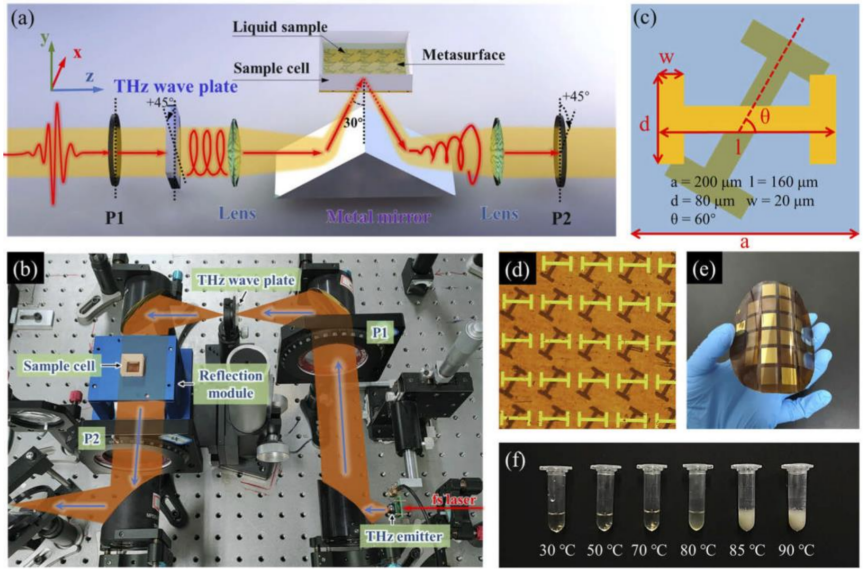

Figure 5. (**a**) Schematic diagram of the THz experimental configuration. (**b**) Photograph of the THz optical path of the experimental setup. (**c**) The geometry of the twisted dual-layer metasurface. (**d**) The micrograph of the metasurface. (**e**) Photograph of double-layer metasurface with the flexible PI substrate. (**f**) The appearance of BSA solution changes with temperature. Reprinted from Ref. [199].

Generally, circular polarization (CP) sensing shows an improvement in the sensitivity and more information sensing, if compared with the traditional linear polarization (LP) spectra. The influence of a double-layer metasurface sensor is proven to enhance also the polarization response of the sample. In fact, nature-conformation proteins are clearly distinguishable, and denaturation induced by temperature treatments can be detected through variations of CP reflection spectra, both right- (RCP) and left-handed (LCP). Compared with the traditional LP spectra, the CP sensing sensitivity is improved. The detection sensitivity achieved with thermal denaturation measurements is established to be Sd = 6.30 dB%, but THz-TDPS reaches a detection sensitivity of Sc = 52.9 dB mL/g for concentration estimations, reported in Figures 6 and 7.

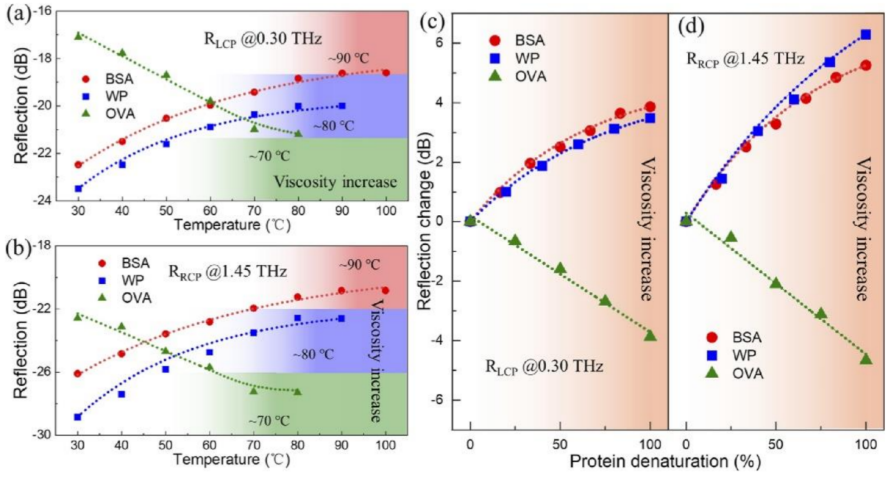

Figure 6. (**a**) The peak values of the R_{LCP} and (**b**) R_{RCP} of BSA, WP and OVA solutions change as a function of the heat-treatment temperature. The temperatures, reported in these two figures, refer to the temperature of the complete denaturation for a certain protein. Relationship of the peak value change of (**c**) R_{LCP} and (**d**) R_{RCP} vs. the denaturation percentage. Reprinted from Ref. [199].

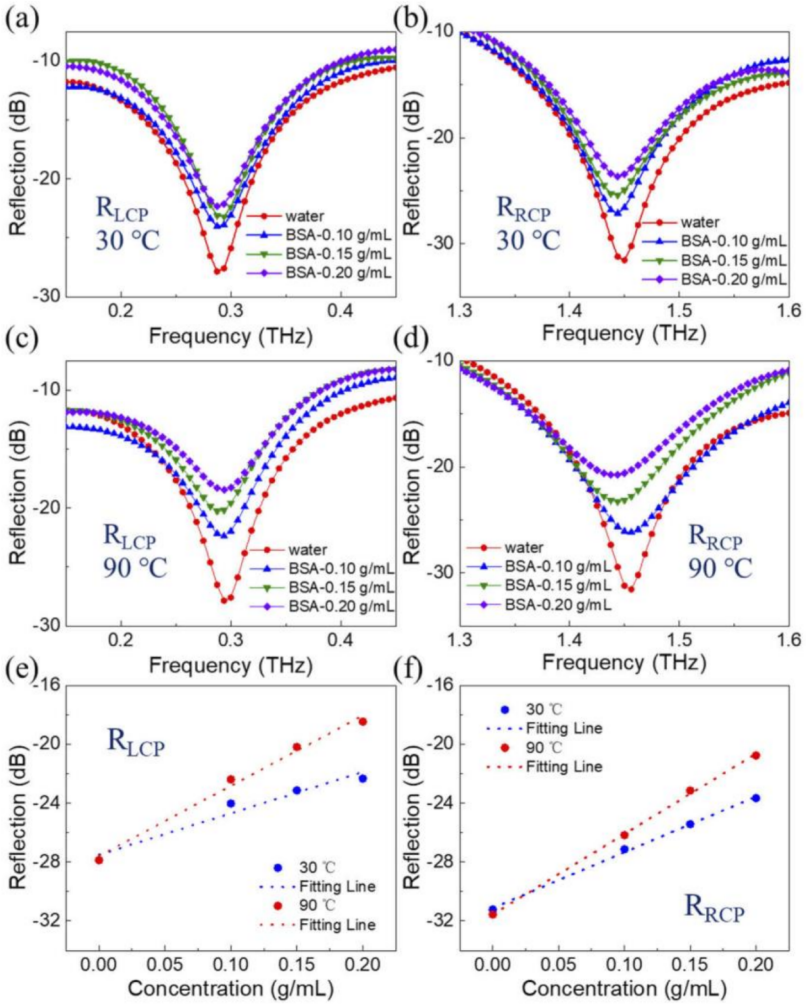

Figure 7. Sensing results of the BSA solution with different concentrations. (**a**) LCP spectra R_{LCP} and (**b**) R_{RCP} at 30 °C. (**c**) R_{LCP} and (**d**) R_{RCP} at 90 °C. The peak value (**e**) R_{LCP} and (**f**) R_{RCP} of BSA solution change with sample concentration. Reprinted from Ref. [199].

Proteins require an environment as close as possible to the living environment, i.e., an aqueous solution. The role of water in protein dynamics has been, and still is, debated. Although water is a limiting factor in THz spectroscopy due to strong absorption in the spectral region of interest, this does not limit protein hydration studies. Combining THz spectroscopy and molecular simulations, Meister's group [200] looked at the behavior of long-range protein–water dynamics in hyperactive insect antifreeze proteins. THz measurements are highly dependent on relative humidity, as protein films have a high affinity for adsorbed water [201]. Heyden and Havenith [202] engaged in both experimental and theoretical study of protein-hydration coupling. Xu et al. [203] measured the absorption spectrum of solvated BSA between 0.3 and 3.72 THz (10–124 cm^{-1}) in order to monitor its collective vibrational dynamics and obtain information in the low-frequency region. They successfully estimated the THz molar absorption of solvated BSA from the much stronger attenuation of water. They deduced that the vibrational modes of solvated proteins lead to a dense and overlapping spectrum monotonously increasing with frequency. The lack of a distinct and spectrally structured spectrum suggested the lack of a specific dominant collective vibration foreseen by molecular dynamics simulations and normal mode analysis of a series of small proteins.

Furthermore, the study of the protein–water interaction can be reported at the cellular level, which turns out to be highly fashionable. In fact, membrane proteins are those that in this context are most involved in the interaction with water, with possible changes in the

structure and the ability to create a network of hydrogen bonds, which can be explored from 1 to 6 THz. Pal and Chattopadhyay [204] probably provided the first and accurate overview of the potential of THz spectroscopy in this area. They demonstrated how THz-TDS and some optical parameters (e.g., the dielectric constant) can describe specific changes in the membrane microenvironment and lipid concentration. The references listed since up to now only emphasize the potential of THz radiation in the field of protein biochemistry. Specifically, the ability of THz spectroscopy to detect the presence of types of proteins, to quantify their content and to be sensitive to protein conformation paves the way for its use in the biomedical and bioclinical fields. Many pathologies are in fact due to an alteration of the aminoacetic sequences and/or functional protein alterations. Recently, Wang et al. [205] exploited time-resolved THz spectroscopy to analyze serum and cerebrospinal fluid (CSF) extracted from rats at different times after blast-induced head injury (bTBI), from both the hypothalamus and the hippocampus.

THz spectra change as a function of time, with different trends for proteins of the hypothalamus and hippocampus. Specifically, Figure 8a,b shows the results of Wang et al. [205], relating to absorption spectra and refractive index between 0.2 and 2.0 THz (6.66–66.6 cm^{-1}) of the total protein in the hypothalamus. The panels showed a magnified area in the range 1–1.6 THz (33.3–53.3 cm^{-1}). Overall, the absorption coefficient and refractive index of total proteins in the hypothalamus rose and fell monotonously as a function of frequency, respectively. To describe the temporal evolution in a clear way, normalized values of optical parameters were selected at 1.6 THz, in Figure 8c. Differences were observed just at 3 h from blast exposure; the absorption coefficients relative to mild and moderate insults were significantly higher than those in the sham group. Subsequently, increasing the time (6 h and 24 h), these values decreased gradually, returning to the normal level, although differences persist between the two parameters also 24 h after the blast exposure.

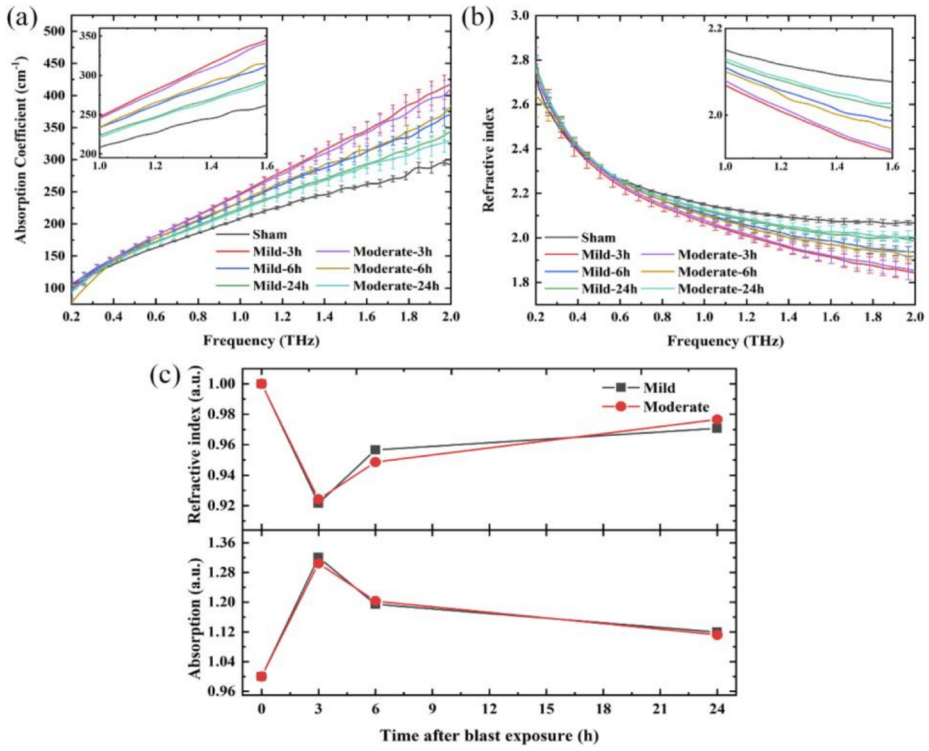

Figure 8. THz spectra of total protein in the hypothalamus. (**a**) Absorption coefficient spectra; (**b**) refractive index spectra; (**c**) the normalized absorption coefficient and refractive index values at 1.6 THz. Reprinted from Ref. [205].

In the same way, THz spectra of the total protein in the hippocampus and its temporal changes are evaluated and are shown in Figure 9a,c. Both the THz absorption and refractive index showed no significant changes 3 h after blast exposure, unlike what happens for the hypothalamus. However, after an additional 3 h, the THz absorption coefficient of the total protein in the hippocampus increases accompanied by a decrease in the refractive index THz, with the increase in the traumatic degree. These changes were more noticeable with the increase in traumatic degree. The bTBI caused some changes in both the hypothalamus and hippocampus total proteins of rats, a behavior associated with the decrease or the increase in the number of some biomolecules with effects on the functioning of brain areas and symptoms of neurological damage. THz technology then appears as a powerful tool for early recognition and diagnosis of bTBI.

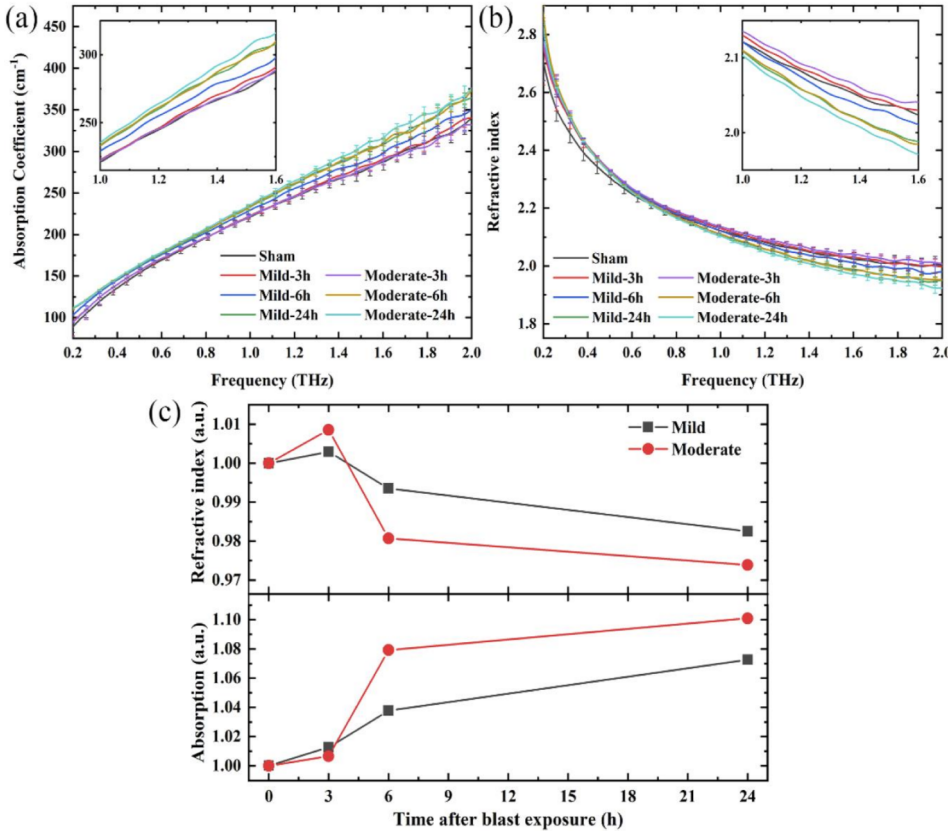

Figure 9. THz spectra of total protein in the hippocampus. (**a**) Absorption coefficient; (**b**) refractive index; (**c**) the normalized absorption coefficient and refractive index values at 1.6 THz. Reprinted from Ref. [205].

6. Conclusions

Proteins play a fundamental role in biology and, in particular, in living systems. The study of the dynamics of proteins provides information on their functionality, catalysis and potential alteration towards pathological diseases and, therefore, are of interest for various research fields.

Various techniques are currently used for their quantification, identification and evolutionary study; still, the demand of new techniques to complement the existing ones is growing. Although various techniques for protein investigation are currently used in the industrial, pharmaceutical and diagnostic fields, limitations, complexity and cost represent serious drawbacks. In this framework, emerging spectroscopic analytical methods, based on the use of THz radiation in the range 0.1–15 THz, are now competitive methods in the biochemical community. Thanks to new technology, the potential of THz spectroscopy has

been affirmed in the analysis of both simple structures, such as polyamide molecules, and complex structures, such as protein complexes.

This short review highlights the possibility of identifying amino acids and proteins and revealing protein dynamics. In the first part we recalled the most common and used techniques from those for the evaluation of protein concentration, the differentiation of proteins and the study of conformational dynamics and modifications. In the second part we focused on THz radiation opportunities outlining issues and applications in which it offers real advantages.

THz spectroscopy provides a unique perspective on the chemical structure, rotational and vibrational molecule modes and intermolecular vibrations, such as hydrogen bonds [102,103]. Furthermore, it is sensitive to the crystalline structure, therefore able to distinguish enantiomers, isotopologists and polymorphisms [134]. Most amino acids have a chiral shape, and THz spectroscopy supports their detection, being particularly useful in the field of pharmaceuticals, where it is able to clearly differentiate between the amino acids and the polypeptide and to monitor protein–ligand interactions.

Protein dynamics analysis shows great potentialities, although there are many studies on the spectral change associated with spontaneous and physico-chemical-induced conformational changes. Some caution must be considered in interpretation of these results. The use of chemical simulations and theoretical approaches based on DFT calculations have limitations, but learning algorithms, neural models and deep learning approaches are viable future approaches, as showed by Sun et al., 2018 [206], which combine machine learning and THz analysis for quantitative protein analysis of BSA, deposited at different concentrations on thin films. The information content of the THz absorption spectra was analyzed with principal component analysis (PCA), spectrum regression analysis (SVR) and maximal information coefficient (MIC) to discriminate frequencies, and machine learning methods proved efficient for the recognition of spectral features. Although different applications of this technology showed great potential, scientific and technological issues still need to be addressed, such as the methodological approach to the analysis of samples in aqueous solutions and the need to increase the sensitivity of the THz signal in the presence of weakly active THz materials.

Author Contributions: Conceptualization, A.D., T.M., R.M. and S.L.; writing—original draft preparation, A.D., T.M., R.M. and S.L.; writing—review and editing, all authors; supervision, S.L.; project administration, S.L., M.P. and A.M.; funding acquisition, S.L., M.P. and A.M. All authors have read and agreed to the published version of the manuscript.

Funding: This research was supported by the Ph.D. funding in the framework of "Programma Operativo Nazionale (PON)—Ricerca e Innovazione 2014–2020—Azione IV.5—Dottorati su tematiche green. We thank for funding BRIC-INAIL project ID12; NATO Science for Peace and Security Programme under grant No. G5889—"SARS-CoV-2 Multi-Messenger Monitoring for Occupational Health & Safety-SARS 3M", LazioInnova "Gruppi di Ricerca 2020" of the POR FESR 2014/2020—A0375-2020-36651 project entitled "DEUPAS -DEterminazione Ultrasensibile di agenti PAtogeni mediante Spettroscopia" and finally FISR-2020 Fondo Integrativo Speciale per la Ricerca, with the project "Monitoraggio multimessaggero e di apprendimento automatico SARS-CoV-2 per la salute e la sicurezza sul lavoro".

Institutional Review Board Statement: Not applicable.

Informed Consent Statement: Not applicable.

Data Availability Statement: Not applicable.

Conflicts of Interest: The authors declare no conflict of interest.

References

1. Moore, M.C. *Introduction to Western Blotting*; Morphosys Ltd.: Oxfordshire, UK, 2009.
2. Gilda, J.E.; Gomes, A.V. Stain-Free total protein staining is a superior loading control to β-actin for Western blots. *Anal. Biochem.* **2013**, *440*, 186–188. [CrossRef]

3. Moritz, C.P.; Marz, S.X.; Reiss, R.; Schulenborg, T.; Friauf, E. Epicocconone staining: A powerful loading control for Western blots. *Proteomics* **2014**, *14*, 162–168. [CrossRef]
4. Baughman, W.E.; Yokus, H.; Balci, S.; Wilbert, D.S.; Kung, P.; Kim, S.M. Observation of Hydrofluoric Acid Burns on Osseous Tissues by Means of Terahertz Spectroscopic Imaging. *IEEE J. Biomed. Health Inform.* **2013**, *17*, 798–805. [CrossRef]
5. Belouzard, S.; Millet, J.K.; Licitra, B.N.; Whittaker, G.R. Mechanism of Coronavirus Cell Entry Mediated by the Viral Spike Protein. *Viruses* **2012**, *4*, 1011–1033. [CrossRef]
6. Verma, J.; Subbarao, N. A comparative study of human betacoronavirus spike proteins: Structure, function and therapeutics. *Arch. Virol.* **2021**, *166*, 697–714. [CrossRef]
7. Whitford, D. *Proteins: Structure and Function*, 1st ed.; Wiley: Chichesetr, UK, 2005.
8. Lesk, A.M. *Introduction to Protein Science: Architecture, Function, and Genomics*, 2nd ed.; Oxford University Press: Oxford, UK, 2010.
9. Fields, P.A. Review: Protein function at thermal extremes: Balancing stability and flexibility. *Comp. Biochem. Physiol. A Mol. Integr. Physiol.* **2001**, *129*, 417–431. [CrossRef]
10. Johan, K. New method for the determination of nitrogen in organic substances. *Z. Anal. Chem.* **1883**, *22*, 366–383.
11. George, W. New decomposition product of urea. *J. Prakt. Chem.* **1847**, *42*, 255–256.
12. Zor, T.; Selinger, Z. Linearization of the Bradford protein assay increases its sensitivity: Theoretical and experimental studies. *Anal. Biochem.* **1996**, *236*, 302–308. [CrossRef]
13. Everette, J.D.; Bryant, Q.M.; Green, A.M.; Abbey, Y.A.; Wangila, G.W.; Walker, R.B. Thorough study of reactivity of various compound classes toward the Folin-Ciocalteu reagent. *J. Agric. Food Chem.* **2010**, *58*, 8139–8144. [CrossRef]
14. Kurien, B.T.; Scofield, R.H. (Eds.) Western Blotting: An Introduction. *Methods Mol. Biol.* **2015**, *1312*, 17–30.
15. Chang, S.K.C. Food analysis. In *Protein Analysis*, 3rd ed.; Nielse, S.S., Ed.; Kluwer Academic: New York, NY, USA, 2003; pp. 131–142.
16. Wilson, P.R. A new instrumentation concept for nitrogen/protein analysis. A challenge to the Kjeldahl method. *Asp. Appl. Biol.* **1990**, *25*, 443–446.
17. Hall, N.G.; Schonfeldt, H.C. Total nitrogen vs. amino-acid profile as indicator of protein content of beef. *Food Chem.* **2013**, *140*, 608–612. [CrossRef]
18. Lee, P.Y.; Costumbrado, J.; Hsu, C.Y.; Kim, Y.H. Agarose gel electrophoresis for the separation of DNA fragments. *J. Vis. Exp.* **2012**, *20*, e3923. [CrossRef]
19. Stellwagen, N.C. Electrophoresis of DNA in agarose gels, polyacrylamide gels and in free solution. *Electrophoresis* **2009**, *30*, S188–S195. [CrossRef]
20. Chattopadhyay, P.K.; Gierahm, T.M.; Roederer, M.; Love, J.C. Single-cell technologies for monitoring immune systems. *Nat. Immunol.* **2014**, *15*, 128–135. [CrossRef]
21. Geering, B.; Fussenegger, M. Synthetic immunology: Modulating the human immune system. *Trends Biotechnol.* **2015**, *33*, 65–79. [CrossRef]
22. Shukla, A.A.; Thommes, J. Recent advances in large-scale production of monoclonal antibodies and related proteins. *Trends Biotechnol.* **2010**, *28*, 253–261. [CrossRef]
23. Tomar, N.; De, R.K. Immunoinformatics: A brief review. *Methods Mol. Biol.* **2014**, *1184*, 23–55.
24. Virgo, P.F.; Gibbs, G.J. Flow cytometry in clinical pathology. *Ann. Clin. Biochem.* **2012**, *49*, 17–28. [CrossRef]
25. Deakin, T. Radisotopic characterization as an analytical tool: Current status, limitations and future challenges. *Bioanalysis* **2015**, *7*, 541–555. [CrossRef]
26. Diao, B.; Wen, K.; Zhang, J.; Chen, J.; Han, C.; Chen, Y.; Wang, S.; Deng, G.; Zhou, H.; Wu, Y. Accuracy of a nucleocapsid protein antigen rapid test in the diagnosis of SARS-CoV-2 infection. *Clin. Microbiol. Infect.* **2021**, *27*, 289.e1–289.e4. [CrossRef]
27. Chen, L.; Zhao, J.; Peng, J.; Li, X.; Deng, X.; Geng, Z.; Shen, Z.; Guo, F.; Zhang, Q.; Jin, Y.; et al. Detection of SARS-CoV-2 in saliva and characterization of oral symptoms in COVID-19 patients. *Cell Prolif.* **2020**, *53*, e12923. [CrossRef]
28. Webb, R.H. Confocal optical microscopy. *Rep. Prog. Phys.* **1996**, *59*, 427–471. [CrossRef]
29. Hoover, E.E.; Squier, J.A. Advances in multiphoton microscopy technology. *Nat. Photonics* **2013**, *7*, 93–101. [CrossRef]
30. Zumbusch, A.; Langbein, W.; Borri, P. Nonlinear vibrational microscopy applied to lipid biology. *Prog. Lipid Res.* **2013**, *52*, 615–632. [CrossRef]
31. D'Arco, A.; Brancati, N.; Ferrara, M.A.; Indolfi, M.; Frucci, M.; Sirleto, L. Subcellular chemical and morphological analysis by stimulated Raman scattering microscopy and image analysis techniques. *Biomed. Opt. Express* **2016**, *7*, 1853–1864. [CrossRef]
32. Cheng, J.X.; Xie, X.S. Vibrational spectroscopic imaging of living systems: An emerging platform for biology and medicine. *Science* **2015**, *50*, 62–64. [CrossRef]
33. D'Arco, A.; Ferrara, M.A.; Indolfi, M.; Tufano, V.; Sirleto, L. Label-free imaging of small lipid droplets by femtosecond-stimulated Raman scattering microscopy. *J. Nonlinear Opt. Phys. Mater.* **2017**, *26*, 1750052. [CrossRef]
34. Min, W.; Freudiger, C.W.; Lu, S.; Xie, X.S. Coherent nonlinear optical imaging: Beyond fluorescence microscopy. *Annu. Rev. Phys. Chem.* **2011**, *62*, 507–530. [CrossRef]
35. Streets, A.M.; Li, A.; Chen, T.; Huang, Y. Imaging without fluorescence: Nonlinear optical microscopy for quantitative cellular imaging. *Anal. Chem.* **2014**, *86*, 8506–8513. [CrossRef]
36. Jepsen, P.U.; Cooke, D.G.; Koch, M. Terahertz spectroscopy and imaging—Modern techniques and applications. *Laser Photonics Rev.* **2011**, *5*, 124–166. [CrossRef]

37. Xie, L.; Gao, W.; Shu, J.; Ying, Y.; Kono, J. Extraordinary sensitivity enhancement by metasurfaces in terahertz detection of antibiotics. *Sci. Rep.* **2015**, *5*, 8671. [CrossRef]
38. Wang, Q.; Ma, Y.H. Qualitative and quantitative identification of nitrogen in terahertz region. *Chemom. Intell. Lab.* **2013**, *127*, 43–48. [CrossRef]
39. Hickman, A.B.; Davies, D.R. Principle of Macromolecular X-ray Crystallography. In *Current Protocols in Protein*; Chapter 17; Science Wiley Interscience: New York, NY, USA, 2001.
40. Lipfert, J.; Doniach, S. Small-angle X-ray scattering from RNA, proteins, and protein complexes. *Annu. Rev. Biophys. Biomol. Struct.* **2007**, *36*, 307–327. [CrossRef]
41. Miao, J.; Ishikawa, T.; Shen, Q.; Earnest, T. Extending X-ray crystallography to allow the imaging of noncrystalline materials, cells, and single protein complexes. *Annu. Rev. Phys. Chem.* **2008**, *59*, 387–410. [CrossRef]
42. Neylon, C. Small angle neutron and X-ray scattering in structural biology: Recent examples from the literature. *Eur. Biophys. J.* **2008**, *37*, 531–541. [CrossRef]
43. Blamire, A.M. The technology of MRI: The next 10 years? *Br. J. Radiol. Suppl.* **2008**, *81*, 601–617. [CrossRef]
44. Ishima, R.; Torchia, D.A. Protein dynamics from NMR. *Nat. Struct. Biol.* **2000**, *7*, 740–743. [CrossRef]
45. McDermott, A.; Polenova, T. Solid state NMR: New tools for insight into enzyme function. *Curr. Opin. Struct. Biol.* **2007**, *17*, 617–622. [CrossRef]
46. Bajar, B.T.; Wang, E.S.; Zhang, S.; Lin, M.Z.; Chu, J. A Guide to Fluorescent Protein FRET Pairs. *Sensors* **2016**, *16*, 1488. [CrossRef]
47. Miura, K. An Overview of Current Methods to Confirm Protein-Protein Interactions. *Protein Pept. Lett.* **2018**, *25*, 72–733. [CrossRef]
48. Dale, N.C.; Johnstone, E.K.M.; White, C.W.; Pfleger, K.D.G. NanoBRET: The Bright Future of Proximity-Based Assays. *Front. Bioeng. Biotechnol.* **2019**, *26*, 56. [CrossRef]
49. Lippincott-Schwartz, J.; Snapp, E.L.; Phair, R.D. The Development and Enhancement of FRAP as a Key Tool for Investigating Protein Dynamics. *Biophys. J.* **2018**, *115*, 1146–1155. [CrossRef]
50. Fasman, G.D. *Circular Dichroism and the Conformational Analysis of Biomolecules*; Plenum Press: New York, NY, USA, 1996.
51. Hofmann, A.; Simon, A.; Grkovic, T.; Jones, M. *Methods of Molecular Analysis in the Life Sciences*; Cambridge University Press: Cambridge, UK, 2014.
52. Pescitelli, G.; Di Bari, L.; Berova, N. Application of electronic circular dichroism in the study of supramolecular systems. *Chem. Soc. Rev.* **2014**, *43*, 5211–5233. [CrossRef]
53. Barth, A. Infrared spectroscopy of proteins. *Biochim. Biophys. Acta Bioenerg.* **2007**, *1767*, 1073–1101. [CrossRef]
54. Marcelli, A.; Cricenti, A.; Kwiatek, W.M.; Petibois, C. Biological applications of synchrotron radiation infrared spectromicroscopy. *Biotech. Adv.* **2012**, *30*, 1390–1404. [CrossRef]
55. Piccirilli, F.; Tardani, F.; D'Arco, A.; Birarda, G.; Vaccari, L.; Sennato, S.; Casciardi, S.; Lupi, S. Infrared Nanospectroscopy Reveals DNA Structural Modifications upon Immobilization onto Clay Nanotubes. *Nanomaterials* **2021**, *11*, 1103. [CrossRef]
56. Auston, D.H.; Nuss, M.C. Electrooptical generation and detection of femtosecond electrical transients. *IEEE J. Quantum Electron.* **1988**, *24*, 184–197. [CrossRef]
57. Mittleman, D.; Gupta, M.; Neelamani, R.; Baraniuk, R.G.; Rudd, J.V.; Koc, M. Recent advances in terahertz imaging. *Appl. Phys. B* **1999**, *68*, 1085–1094. [CrossRef]
58. Siegel, P.H. Terahertz technology in biology and medicine. *IEEE Trans. Microw. Theory* **2004**, *52*, 2438–2447. [CrossRef]
59. Zhang, X.C. Terahertz wave imaging: Horizons and hurdles. *Phys. Med. Biol.* **2002**, *47*, 3667–3677. [CrossRef]
60. Wallace, V.P.; Taday, P.F.; Fitzgerald, A.J.; Woodward, R.M.; Cluff, J.; Pye, R.J.; Arnone, D.D. Terahertz pulsed imaging and spectroscopy for biomedical and pharmaceutical applications. *Faraday Discuss.* **2004**, *126*, 255–263. [CrossRef]
61. Withayachumnankul, W.; Png, G.M.; Yin, X.; Atakaramians, S.; Jones, I.; Lin, H.; Ung, B.S.Y.; Balakrishnan, J.; Ng, B.W.-H.; Ferguson, B.; et al. T-ray sensing and imaging. *Proc. IEEE* **2007**, *95*, 1528–1558. [CrossRef]
62. Cheon, H.; Yang, H.J.; Son, J.-H. Toward Clinical Cancer Imaging Using Terahertz Spectroscopy. *IEEE J. Sel. Top. Quantum Electron.* **2017**, *23*, 8600109. [CrossRef]
63. Mickan, S.; Abbott, D.; Munchb, J.; Zhang, X.C.; van Doornd, T. Analysis of system trade-offs for terahertz imaging. *Microelectron. J.* **2000**, *31*, 503–514. [CrossRef]
64. Mou, S.; D'Arco, A.; Tomarchio, L.; Di Fabrizio, M.; Curcio, A.; Lupi, S.; Petrarca, M. Simultaneous elliptically and radially polarized THz from one-color laser-induced plasma filament. *New J. Phys.* **2021**, *23*, 063048. [CrossRef]
65. Curcio, A.; Petrarca, M. Diagnosing plasmas with wideband terahertz pulses. *Opt. Lett.* **2019**, *44*, 1011–1014. [CrossRef]
66. Curcio, A.; Dolci, V.; Lupi, S.; Petrarca, M. Terahertz-based retrieval of the spectral phase and amplitude of ultrashort laser pulses. *Opt. Lett.* **2018**, *43*, 783–786. [CrossRef]
67. Curcio, A.; Marocchino, A.; Dolci, V.; Lupi, S.; Petrarca, M. Resonant plasma excitation by single-cycle THz pulses. *Sci. Rep.* **2018**, *8*, 1052. [CrossRef]
68. Curcio, A.; Mou, S.; Palumbo, L.; Lupi, S.; Petrarca, M. Selection rules for the orbital angular momentum of optically produced THz radiation. *Opt. Lett.* **2021**, *46*, 1514–1517. [CrossRef]
69. D'Arco, A.; Tomarchio, L.; Dolci, V.; Di Pietro, P.; Perucchi, A.; Mou, S.; Petrarca, M.; Lupi, S. Broadband Anisotropic Optical Properties of the Terahertz Generator HMQ-TMS Organic Crystal. *Condens. Matter* **2020**, *5*, 47. [CrossRef]
70. Lupi, S.; Molle, A. Emerging Dirac materials for THz plasmonics. *Appl. Mater. Today* **2020**, *20*, 100732. [CrossRef]

71. Di Pietro, P.; Ortolani, M.; Limaj, O.; Di Gaspare, A.; Giliberti, V.; Giorgianni, F.; Brahlek, M.; Bansal, N.; Koirala, N.; Oh, S.; et al. Observation of Dirac plasmons in a topological insulator. *Nat. Nanotechnol.* **2013**, *8*, 556–560. [CrossRef]
72. D'Apuzzo, F.; Piacenti, A.R.; Giorgianni, F.; Autore, M.; Cestelli Guidi, M.; Marcelli, A.; Schade, U.; Ito, Y.; Chen, M.; Lupi, S. Terahertz and mid-infrared plasmons in three-dimensional nanoporous graphene. *Nat. Commun.* **2017**, *8*, 14885. [CrossRef]
73. Giorgianni, F.; Chiadroni, E.; Rovere, A.; Cestelli-Guidi, M.; Perucchi, A.; Bellaveglia, M.; Castellano, M.; Di Giovenale, D.; Di Pirro, G.; Ferrario, M.; et al. Strong nonlinear terahertz response induced by Dirac surface states in Bi2Se3 topological insulator. *Nat. Commun.* **2016**, *7*, 11421. [CrossRef]
74. Marcelli, A.; Irizawa, A.; Lupi, S. THz: Research frontiers for new sources, imaging and other advanced technologies. *Condens. Matter* **2019**, *6*, 23.
75. Galstyan, V.; D'Arco, A.; Di Fabrizio, M.; Poli, N.; Lupi, S.; Comini, E. Detection of volatile organic compounds: From chemical gas sensors to terahertz spectroscopy. *Rev. Anal. Chem.* **2021**, *40*, 33–57. [CrossRef]
76. Naftaly, M.; Vieweg, N.; Deninger, A. Industrial Applications of Terahertz Sensing: State of Play. *Sensors* **2019**, *19*, 4203. [CrossRef]
77. Choi, J.; Ryu, S.Y.; Kwon, W.S.; Kim, K.S.; Kim, S. Compound Explosives Detection and Component Analysis via Terahertz Time-Domain Spectroscopy. *Korean J. Opt. Photonics* **2013**, *17*, 454–460. [CrossRef]
78. Smith, R.M.; Arnold, M.A. Selectivity of Terahertz Gas-Phase Spectroscopy. *Anal. Chem.* **2015**, *87*, 10679–10683. [CrossRef]
79. Rothbart, N.; Holz, O.; Koczulla, R.; Schmalz, K.; Hübers, H.W. Analysis of Human Breath by millimeter-Wave/Terahertz Spectroscopy. *Sensors* **2019**, *19*, 2719. [CrossRef]
80. Giuliano, B.M.; Gavdush, A.A.; Müller, B.; Zaytsev, K.I.; Grassi, T.; Ivlev, A.V.; Palumbo, M.E.; Baratta, G.A.; Scirè, C.; Komandin, G.A.; et al. Broadband spectroscopy of astrophysical ice analogues I. Direct measurement of the complex refractive index of CO ice using terahertz time-domain spectroscopy. *Astron. Astrophys.* **2019**, *629*, A112. [CrossRef]
81. D'Arco, A.; Di Fabrizio, M.; Dolci, V.; Marcelli, A.; Petrarca, M.; Della Ventura, G.; Lupi, S. Characterization of volatile organic compounds (VOCs) in their liquid-phase by terahertz time-domain spectroscopy. *Biomed. Opt. Express* **2020**, *11*, 1–7. [CrossRef]
82. Fischer, B.; Hoffmann, M.; Helm, H.; Modjesch, G.; Uhd Jepsen, P. Chemical recognition in terahertz time-domain spectroscopy and imaging. *Semicond. Sci. Technol.* **2005**, *20*, S246. [CrossRef]
83. Stoik, C.D.; Bohn, M.J.; Blackshire, J.L. Nondestructive evaluation of aircraft composites using transmissive terahertz time domain spectroscopy. *Opt. Express* **2008**, *16*, 17039–17051. [CrossRef]
84. Heimbeck, M.S.; Ng, W.R.; Golish, D.R.; Gehm, M.E.; Everitt, H.O. Terahertz digital holographic imaging of voids within visibly opaque dielectrics. *IEEE Trans. Terahertz Sci. Technol.* **2015**, *5*, 110–116. [CrossRef]
85. Tomarchio, L.; Macis, S.; D'Arco, A.; Mou, S.; Grilli, A.; Romani, M.; Cestelli Guidi, M.; Hu, K.; Kukunuri, S.; Jeong, S.; et al. Disordered photonics behavior from terahertz to ultraviolet of a three-dimensional graphene network. *NPG Asia Mater.* **2021**, *13*, 73. [CrossRef]
86. Federici, J.F.; Schulkin, B.; Huang, F.; Gary, D.; Barat, R.; Oliveira, F.; Zimdars, D. THz imaging and sensing for security applications—Explosives, weapons and drugs. *Semicond. Sci. Technol.* **2005**, *20*, S266. [CrossRef]
87. Ergün, S.; Sönmez, S. Terahertz Technology for Military Applications. *J. Assoc. Inf. Sci. Technol.* **2015**, *3*, 13–16. [CrossRef]
88. Liu, H.B.; Zhong, H.; Karpowicz, N.; Chen, Y.; Zhang, X.C. Terahertz spectroscopy and imaging for defense and security applications. *Proc. IEEE* **2007**, *95*, 1514–1527. [CrossRef]
89. D'Arco, A.; Mussi, V.; Petrov, S.; Tofani, S.; Petrarca, M.; Beccherelli, R.; Dimitrov, D.; Marinova, V.; Lupi, S.L.; Zografopoulos, D.C. Fabrication and spectroscopic characterization of graphene transparent electrodes on flexible cyclo-olefin substrates for terahertz electro-optic applications. *Nanotechnology* **2020**, *31*, 364006. [CrossRef]
90. Wang, K.; Sun, D.W.; Pu, H. Emerging non-destructive terahertz spectroscopic imaging technique: Principle and applications in the agri-food industry. *Trend Food Sci. Technol.* **2017**, *67*, 93–105. [CrossRef]
91. Cosentino, A. Terahertz and cultural heritage science: Examination of art and archeology. *Technologies* **2016**, *4*, 6. [CrossRef]
92. Yamaguchi, S.; Yamaguchi, S.; Fukushi, Y.; Kubota, O.; Itsuji, T.; Ouchi, T.; Yamamoto, S. Brain tumor imaging of rat fresh tissue using terahertz spectroscopy. *Sci. Rep.* **2016**, *6*, 30124. [CrossRef]
93. Bajwa, N.; Au, J.; Jarrahy, R.; Sung, S.; Fishbein, M.C.; Riopelle, D.; Ennis, D.B.; Aghaloo, T.; John, M.A.; Grundfest, W.S.; et al. Non-invasive terahertz imaging of tissue water content for flap viability assessment. *Biomed. Opt. Express* **2017**, *8*, 460–474. [CrossRef]
94. Zaytsev, I.; Dolganova, I.N.; Chernomyrdin, N.V.; Katyba, G.M.; Gavdush, A.A.; Cherkasova, O.P.; Komandin, G.A.; Shchedrina, M.A.; Khodan, A.N.; Ponomarev, D.S.; et al. The progress and perspectives of terahertz technology for diagnosis of neoplasms: A review. *J. Opt.* **2020**, *22*, 013001. [CrossRef]
95. Yang, X.; Zhao, X.; Yang, K.; Liu, Y.; Liu, Y.; Fu, W.; Luo, Y. Biomedical Applications of Terahertz Spectroscopy and Imaging. *Trends Biotechnol.* **2016**, *34*, 810–824. [CrossRef]
96. Son, J.H.; Oh, S.J.; Cheon, H. Potential clinical applications of terahertz radiation. *J. Appl. Phys.* **2019**, *125*, 190901. [CrossRef]
97. D'Arco, A.; Di Fabrizio, M.; Dolci, V.; Petrarca, M.; Lupi, S. THz Pulsed Imaging in Biomedical Applications. *Condens. Matter* **2020**, *5*, 25. [CrossRef]
98. Di Fabrizio, M.; D'Arco, A.; Mou, S.; Palumbo, L.; Petrarca, M.; Lupi, S. Performance Evaluation of a THz pulsed Imaging System: Point Spread Function, Broadband THz Beam Visualization and Image Reconstruction. *Appl. Sci.* **2021**, *11*, 562. [CrossRef]
99. Di Fabrizio, M.; Lupi, S.; D'Arco, A. Virus recognition with terahertz radiation: Drawbacks and potentialities. *J. Phys. Photonics* **2021**, *3*, 032001. [CrossRef]

100. Lee, Y.S. *Principles of Terahertz Science and Technology*; Springer: Berlin/Heidelberg, Germany, 2009.
101. Zhang, X.C.; Xu, J. *Introduction to THz Wave Photonics*; Springer: Berlin/Heidelberg, Germany, 2010.
102. Walther, M.; Plochocka, P.; Fischer, B.; Helm, H.; Jepsen, P.U. Collective Vibrational Modes in Biological Molecules Investigated by Terahertz Time-domain Spectroscopy. *Biopolymers* **2002**, *67*, 310–313. [CrossRef]
103. Tanabe, T.; Watanabe, K.; Oyama, Y.; Seo, K. Polarization Sensitive THz Absorption Spectroscopy for the Evaluation of Uniaxially Deformed Ultra-high Molecular Weight Polyethylene. *NDT & E Int.* **2010**, *43*, 329–333.
104. Parrott, E.P.J.; Zeitler, J.A. Terahertz Time-Domain and Low-Frequency Raman Spectroscopy of Organic Materials. *Appl. Spectrosc.* **2015**, *69*, 1–25. [CrossRef]
105. Cooksey, C.C.; Greer, B.J.; Heilweil, E.J. Terahertz Spectroscopy of L-Proline in Reverse Aqueous Micelles. *Chem. Phys. Lett.* **2009**, *467*, 424–429. [CrossRef]
106. Yue, W.; Wang, W.; Zhao, G.; Zhang, C.; Yan, H. THz Spectrum of Aromatic Amino Acid. *Chin. Phys. Soc.* **2005**, *54*, 3094–3099.
107. Kutteruf, M.R.; Brown, C.M.; Iwaki, L.K.; Campbell, M.B.; Korter, T.M.; Heilweil, E.J. Terahertz spectroscopy of short-chain polypeptides. *Chem. Phys. Lett.* **2003**, *375*, 337–343. [CrossRef]
108. Manti, L.; D'Arco, A. Cooperative biological effects between ionizing radiation and other physical and chemical agents. *Mutat. Res.* **2010**, *704*, 115–122. [CrossRef]
109. Lee, D.-K.; Kang, J.-H.; Know, J.; Lee, J.-S.; Lee, S.; Woo, D.H.; Kim, J.H.; Song, C.-S.; Park, Q.H.; Seo, M. Nano metamaterials for ultrasensitive terahertz biosensing. *Sci. Rep.* **2017**, *7*, 8146. [CrossRef]
110. Lin, H.; Withayachumnankul, W.; Fischer, B.; Mickan, S.; Abbott, D. Gas recognition with terahertz time-domain spectroscopy and spectral catalog: A preliminary study. *Terahertz Photonics* **2008**, *6840*, 68400X.
111. Kindt, J.T.; Schmuttenmaer, C.A. Far-Infrared Dielectric Properties of Polar Liquids Probed by Femtosecond Terahertz Pulse Spectroscopy. *J. Phys. Chem.* **1996**, *100*, 10373–10379. [CrossRef]
112. Fedulova, E.; Nazarov, M.; Angeluts, A.; Kitai, M.; Sokolov, V.; Shkurinov, A. Studying of dielectric properties of polymers in the terahertz frequency range. In *Optical technologies in biophysics and medicine XIII, Proceedings of the Saratov Fall Meeting 2011, Saratov, Russia, 27–30 September 2011*; SPIE: Bellingham, WA, USA, 2011.
113. Rezvani, S.J.; Di Gioacchino, D.; Tofani, S.; D'Arco, A.; Ligi, C.; Lupi, S.; Gatti, C.; Cestelli Guidi, M.; Marcelli, A. A cryogenic magneto-optical device for long wavelength radiation. *Rev. Sci. Instrum.* **2020**, *91*, 075103. [CrossRef]
114. Burford, N.; El-Shenawee, M.O. Review of terahertz photoconductive antenna technology. *Opt. Eng.* **2017**, *56*, 010901. [CrossRef]
115. Dexheimer, S.L. *Terahertz Spectroscopy: Principles and Applications*; CRC Press: Boca Raton, FL, USA, 2017.
116. Naftaly, M. *Terahertz Metrology*; Artech House: London, UK, 2015.
117. Seo, M.; Park, H.-R. Terahertz Biochemical Molecules-specific sensors. *Adv. Opt. Mater.* **2019**, *8*, 1900662. [CrossRef]
118. Korter, T.M.; Balu, R.; Campbell, M.B.; Beard, M.C.; Gregurick, S.K.; Heilweil, E.J. Terahertz Spectroscopy of Solid Serine and Cysteine. *Chem. Phys. Lett.* **2006**, *418*, 65–70. [CrossRef]
119. Wang, X.; Wang, W. Terahertz Time-domain Spectroscopy of Sulfur-containing Amino Acids. *Acta Chim. Sin.* **2008**, *66*, 2248–2252.
120. Yamamoto, K.; Kabir, M.H.; Tominaga, K. Terahertz Time-domain Spectroscopy of Sulfur-containing Biomolecules. *J. Opt. Soc. Am. B* **2005**, *22*, 2417–2426. [CrossRef]
121. Matei, A.; Drichko, N.; Gompf, B.; Dressel, M. Far-infrared Spectra of Amino Acids. *Chem. Phys.* **2005**, *316*, 61–71. [CrossRef]
122. Wang, W.; Li, H.; Zhang, Y.; Zhang, C. Correlations Between Terahertz Spectra and Molecular Structures of 20 Standard α-Amino Acids. *Acta Phys. Chim. Sin.* **2009**, *25*, 2074–2079.
123. Yan, Z.; Hou, D.; Huang, P.; Cao, B.; Zhang, G.; Zhou, Z. Terahertz Spectroscopic Investigation of L-Glutamic Acid and L-Tyrosine. *Meas. Sci. Technol.* **2008**, *19*, 15602–15605. [CrossRef]
124. Wang, G.; Wang, W. Experimental and Theoretical Investigations on the Terahertz Vibrational Spectroscopy of Alanine Crystal. *Acta Phys. Chim. Sin.* **2012**, *28*, 1579–1585.
125. Zheng, Z.; Fan, W. First Principles Investigation of L-Alanine in Terahertz Region. *Biol. Phys.* **2012**, *38*, 405–413. [CrossRef]
126. Taulbee, A.R.; Heuser, J.A.; Spendel, W.U.; Pacey, G.E. Qualitative Analysis of Collective Mode Frequency Shifts in L-Alanine Using Terahertz Spectroscopy. *Anal. Chem.* **2009**, *81*, 2664–2667. [CrossRef]
127. Taday, P.F.; Bradley, I.V.; Arnone, D.D. Terahertz Pulse Spectroscopy of Biological Materials L-Glutamic Acid. *J. Biol. Phys.* **2003**, *29*, 109–115. [CrossRef]
128. Darkwah, J.; Smith, G.; Ermolina, I.; Mueller-Holtz, M. A THz Spectroscopy Method for Quantifying the Degree of Crystallinity in Freeze-dried Gelatin/Amino Acid Mixtures: An Application for the Development of Rapidly Disintegrating Tablets. *Int. J. Pharm.* **2013**, *455*, 357–364. [CrossRef]
129. Li, Z.; Zhang, Z.; Zhao, X.; Su, H.; Yan, F. Extracting THz Absorption Coefficient Spectrum Based on Accurate Determination of Sample Thickness. *Spectrosc. Spect. Anal.* **2012**, *32*, 1043–1046.
130. Yang, J.; Li, S.; Zhao, H.; Zhang, J.; Yang, N.; Jing, D.; Wang, C.; Han, J. Terahertz Study of L-Asparagine and Its Monohydrate. *Acta Phys. Sin.* **2014**, *63*, 133203. [CrossRef]
131. Nishizawa, J.; Tanno, T.; Yoshida, T.; Suto, K. Consequence of a Defect on the Terahertz Spectra of L-Asparagine Monohydrate. *Chem. Lett.* **2007**, *36*, 134–135. [CrossRef]
132. Chiba, M.; Derreumaux, P.; Vergoten, G. The Use of the Spasiba Spectroscopic Potential for Reproducing the Structures and Vibrational Frequencies of a Series of Acids—Acetic-Acid, Pivalic Acid, Succinic Acid, Adipic Acid And L-Glutamic Acid. *J. Mol. Struct.* **1994**, *317*, 171–184. [CrossRef]

133. Yi, W.; Yu, J.; Xu, Y.; Wang, F.; Yu, Q.; Sun, H.; Xu, L.; Liu, Y.; Jiang, L. Broadband terahertz spectroscopy of amino acids. *Instrum. Sci. Technol.* **2017**, *45*, 423–439.
134. Hufnagle, D.C.; Taulbee-Combs, A.R.; Spendel, W.U.; Pacey, G.E. Collective mode frequency shifts in L-serine and a series of isotopologues in the terahertz regime. *Talanta* **2012**, *88*, 61–65. [CrossRef]
135. Patil, M.R.; Ganorkar, S.B.; Patil, A.S.; Shirkhedkar, A.A. Terahertz Spectroscopy: Encoding the Discovery, Instrumentation, and Applications toward Pharmaceutical Prospectives. *Crit. Rev. Anal. Chem.* **2020**, 1–13. [CrossRef]
136. Williams, M.R.C.; Aschaffenburg, D.J.; Ofori-Okai, B.K.; Schmuttenmaer, C.A. Intermolecular vibrations in hydrophobic amino acid crystals: Experiments and calculations. *J. Phys. Chem. B* **2013**, *117*, 10444–10461. [CrossRef]
137. King, M.D.; Hakey, P.M.; Korter, T.M. Discrimination of chiral solids: A terahertz spectroscopic investigation of l- and dl-serine. *J. Phys. Chem. A* **2010**, *114*, 2945–2953. [CrossRef]
138. Frommel, C. The apolar surface area of amino acids and its empirical correlation with hydrophobic free energy. *J. Theor. Biol.* **1984**, *111*, 247–260. [CrossRef]
139. Kyte, J.; Doolittle, R.F. A simple method for displaying the hydropathic character of a protein. *J. Mol. Biol.* **1982**, *157*, 105–132. [CrossRef]
140. Acharya, H.; Vembanur, S.; Jamadagni, S.N.; Garde, S. Mapping hydrophobicity at the nanoscale: Applications to heterogeneous surfaces and proteins. *Faraday Discuss.* **2010**, *146*, 353–365. [CrossRef]
141. Jensen, J.H.; Gordon, M.S. On the number of water molecules necessary to stabilize the glycine zwitterion. *J. Am. Chem. Soc.* **1995**, *117*, 8159–8170. [CrossRef]
142. Gontrani, L.; Mennucci, B.; Tomasi, J. Glycine and alanine: A theoretical study of solvent effects upon energetics and molecular response properties. *J. Mol. Struct. THEOCHEM* **2000**, *500*, 113–127. [CrossRef]
143. Niehues, G.; Heyden, M.; Schmidt, D.A.; Havenith, M. Exploring hydrophobicity by THz absorption spectroscopy of solvated amino acids. *Faraday Discuss.* **2011**, *150*, 193. [CrossRef] [PubMed]
144. Gordon, M.S.; Jensen, J.H. Understanding the hydrogen bond using quantum chemistry. *Acc. Chem. Res.* **1996**, *29*, 536–543. [CrossRef]
145. Hecht, D.; Tadesse, L.; Walters, L. Correlating hydration shell structure with amino acid hydrophobicity. *J. Am. Chem. Soc.* **1993**, *115*, 3336–3337. [CrossRef]
146. Ide, M.; Maeda, Y.; Kitano, H. Effect of hydrophobicity of amino acids on the structure of water. *J. Phys. Chem. B* **1997**, *101*, 7022–7026. [CrossRef]
147. Qvist, J.; Halle, B. Thermal signature of hydrophobic hydration dynamics. *J. Am. Chem. Soc.* **2008**, *130*, 10345–10353. [CrossRef]
148. Balabin, R.M. The First Step in Glycine Solvation: The Glycine−Water Complex. *J. Phys. Chem. B* **2010**, *114*, 15075–15078. [CrossRef] [PubMed]
149. McLain, S.E.; Soper, A.K.; Terry, A.E.; Watts, A. Structure and Hydration of L-Proline in Aqueous Solutions. *J. Phys. Chem. B* **2007**, *111*, 4568–4580. [CrossRef] [PubMed]
150. Pacios, L.F. Distinct molecular surfaces and hydrophobicity of amino acid residues in proteins. *J. Chem. Inf. Comput. Sci.* **2001**, *41*, 1427–1435. [CrossRef]
151. Sato, T.; Buchner, R.; Fernandez, S.; Chiba, A.; Kunz, W. Dielectric relaxation spectroscopy of aqueous amino acid solutions: Dynamics and interactions in aqueous glycine. *J. Mol. Liq.* **2005**, *117*, 93–98. [CrossRef]
152. Rodriguez-Arteche, I.; Cerveny, S.; Alegrıa, A.; Colmenero, J. Dielectric spectroscopy in the GHz region on fully hydrated zwitterionic amino acids. *Phys. Chem. Chem. Phys.* **2012**, *14*, 11352–11362. [CrossRef]
153. Suzuki, M.; Shigematsu, J.; Fukunishi, Y.; Kodama, T. Hydrophobic hydration analysis on amino acid solutions by the microwave dielectric method. *J. Phys. Chem. B* **1997**, *101*, 3839–3845. [CrossRef]
154. Bian, Y.; Zhang, X.; Zhu, Z.; Yang, B. Vibrational modes optimization and terahertz time-domain spectroscopy of L-Lysine and L-Lysine hydrate. *J. Mol. Struct.* **2021**, *1232*, 129952. [CrossRef]
155. Morgante, P.; Peverati, R. The devil in the details: Atutorial review on some undervalued aspects of density functional theory calculations. *Int. J. Quant. Chem.* **2020**, *120*, e26332. [CrossRef]
156. Fox, S.J.; Dziedzic, J.; Fox, T.; Tautermann, C.S.; Skylaris, C.K. Density functional theory calculations on entire proteins for free energies of binging: Application to a model polar binding site. *Proteins* **2014**, *82*, 3335–3346. [CrossRef] [PubMed]
157. Pan, T.; Li, S.; Zou, T.; Yu, Z.; Zhang, B.; Wang, C.; Zhang, J.; He, M.; Zhao, H. Terahertz spectra of L-phenylalanine and its monohydrate. *Spectrochim. Acta A Mol. Biomol. Spectrosc.* **2017**, *178*, 19–23. [CrossRef]
158. Samanta, N.; Mahanta, D.S.; Choudhury, S.; Barman, A.; Mitra, R.K. Collective hydration dynamics in some amino acid solutions: A combined GHz-THz spectroscopic study. *J. Chem. Phys.* **2017**, *146*, 125101. [CrossRef]
159. Itoh, K.; Shimanouchi, T. Far-infrared spectra of *N*-methylacetamide and related compounds and hydrogen-bond force constraints. *Biopolymers* **1965**, *5*, 921–930. [CrossRef]
160. Yamamoto, K.; Tominaga, K.; Sasakawa, H.; Tamura, A.; Murakami, H. Terahertz time-domain spectroscopy of amino acids and polypeptides. *Biophys. J.* **2005**, *89*, L22–L24. [CrossRef]
161. Neu, J.; Stone, E.A.; Spies, J.A.; Storch, G.; Hatano, A.S.; Mercado, B.Q.; Miller, S.J.; Schmutternmaer, C.A. Terahertz Spectroscopy of Tetrameric Peptides. *CA J. Phys. Chem. Lett.* **2019**, *10*, 2624–2628. [CrossRef]
162. Yoneyama, H.; Yamashita, M.; Kasai, S.; Kawase, K.; Ueno, R.; Ito, H.; Ouchi, T. Terahertz spectroscopy of native-conformation and thermally denatured bovine serum albumin (BSA). *Phys. Med. Biol.* **2008**, *53*, 3543–3549. [CrossRef]

163. Xie, L.; Yao, Y.; Ying, Y. The application of terahertz spectroscopy to protein detection: A review. *Appl. Spectrosc. Rev.* **2014**, *49*, 448–461. [CrossRef]
164. Sun, Y.; Zhang, Y.; Pickwell-Macpherson, E. Investigating antibody interactions with a polar liquid using terahertz pulsed spectroscopy. *Biophys. J.* **2011**, *100*, 225–231. [CrossRef] [PubMed]
165. Falconer, R.J.; Markelz, A.G. Terahertz spectroscopic analysis of peptides and proteins. *J. Infrared Millim. Terahertz Waves* **2012**, *33*, 973–988. [CrossRef]
166. Cao, C.; Zhang, Z.; Zhao, X.; Zhang, T. Terahertz spectroscopy and machine learning algorithm for non-destructive evaluation of protein conformation. *Opt. Quantum Electron.* **2020**, *52*, 225. [CrossRef]
167. Markelz, A.G.; Roitberg, A.; Heilweil, E.J. Pulsed terahertz spectroscopy of DNA, bovine serum albumin and collagen between 0.1 and 2.0 THz. *Chem. Phys. Lett.* **2000**, *320*, 42–48. [CrossRef]
168. Markelz, A.; Whitmire, S.; Hillebrecht, J.; Birge, R. THz time domain spectroscopy of biomolecular conformational modes. *Phys. Med. Biol.* **2002**, *47*, 3797–3805. [CrossRef] [PubMed]
169. Paciaroni, A.; Orecchini, A.; Haertlein, M.; Moulin, M.; Nibali, V.C.; Francesco, A.D.; Petrillo, C.; Sacchetti, F. Vibrational collective dynamics of dry proteins in the terahertz region. *J. Phys. Chem. B* **2012**, *116*, 3861–3865. [CrossRef]
170. Sun, Y.; Zhong, J.; Zhang, C.; Zuo, J.; Pickwell-MacPherson, E. Label-free detection and characterization of the binding of hemagglutinin protein and broadly neutralizing monoclonal antibodies using terahertz spectroscopy. *J. Biomed. Opt.* **2015**, *20*, 037006. [CrossRef]
171. Castro-Camus, E.; Johnston, M.B. Conformational changes of photoactive yellow protein monitored by terahertz spectroscopy. *Chem. Phys. Lett.* **2008**, *455*, 289–292. [CrossRef]
172. Markelz, A.G. Terahertz dielectric sensitivity to biomolecular structure and function. *IEEE J. Sel. Top. Quantum Electron.* **2008**, *14*, 180–190. [CrossRef]
173. George, D.K.; Knab, J.R.; He, Y.; Kumauchi, M.; Birge, R.R.; Hoff, W.D.; Markelz, A.G. Photoactive yellow protein terahertz response: Hydration, heating and intermediate states. *IEEE Trans. Terahertz Sci. Technol.* **2013**, *3*, 288–294. [CrossRef]
174. Han, X.; Yan, S.; Zang, Z.; Wie, D.; Cui, H.-L.; Du, C. Label-free protein detection using terahertz time-domain spectroscopy. *Biomed. Opt. Express* **2018**, *9*, 994–1005. [CrossRef] [PubMed]
175. Chen, J.Y.; Knab, J.R.; Cerne, J.; Markelz, A.G. Large oxidation dependence observed in terahertz dielectric response for cytochrome c. *Phys. Rev. E* **2005**, *72*, 04090. [CrossRef] [PubMed]
176. Brooks, B.; Karplus, M. Process analytical chemistry: Applications of near infrared spectrometry in environmental and food analysis: An overview. *Proc. Natl. Acad. Sci. USA* **1985**, *82*, 4995. [CrossRef] [PubMed]
177. Kauzmannk, W. Some factors in the interpretation of protein denaturation. *Adv. Protein Chem.* **1959**, *14*, 1–63.
178. Murphy, K.P. Stabilization of protein structure. *Methods Mol. Biol.* **2001**, *168*, 1–16.
179. Freier, E. Thermal denaturation methods in the study of protein folding. *Methods Enzymol.* **1995**, *259*, 144–168.
180. Wijayanti, H.B.; Bansal, N.; Deeth, H.C. Stability of whey proteins during thermal processing: A review. *Compr. Rev. Food Sci. F* **2014**, *13*, 1235–1251. [CrossRef]
181. Wang, B.; Timilsena, Y.P.; Blanch, E.; Adhikari, B. Lactoferrin: Structure, function, denaturation and digestion. *Crit. Rev. Food Sci. Nutr.* **2019**, *59*, 580–596. [CrossRef]
182. Silva, J.L. Pressure stability of proteins. *Annu. Rev. Phys. Chem.* **1993**, *44*, 89–113. [CrossRef]
183. Chirgadze, Y.N.; Ovsepyan, A.M. Observation of small conformational changes in sperm-whale myoglobin by far-infrared spectra. *Biopolymers* **1973**, *12*, 637–645. [CrossRef]
184. Chen, H.; Chen, G.; Li, S.; Wang, L. Reversible conformational change of PsbO Protein detected by terahertz time-domain spectroscopy. *Chin. Phys. Lett.* **2009**, *26*, 084204.
185. Chen, H.; Wang, L.; Qu, Y.G.; Kuang, T.Y.; Li, L.B.; Peng, W.X. Investigation of guanidine hydrochloride induced chlorophyll protein 43 and 47 denaturation in the terahertz frequency range. *J. Appl. Phys.* **2007**, *102*, 074701. [CrossRef]
186. Qu, Y.; Chen, H.; Qin, X.; Wang, L.; Li, L.; Kuang, T. The guanidine hydrochloride-induced denaturation of CP43 and CP47 studied by terahertz time-domain spectroscopy. *Sci. China C Life Sci.* **2007**, *50*, 350–355. [CrossRef] [PubMed]
187. Qu, Y.; Chen, H.; Qin, X.; Li, L.; Wang, L.; Kuang, T. Thermal denaturation of CP43 studied by Fourier transform-infrared spectroscopy and terahertz time-domain spectroscopy. *J. Proteins Proteom.* **2007**, *1774*, 1614–1618. [CrossRef]
188. He, Y.F.; Pei, P.I.; Knab, J.R.; Chen, J.Y.; Markelz, A.G. Protein dynamical transition does not require protein structure. *Phys. Rev. Lett.* **2008**, *101*, 178103. [CrossRef] [PubMed]
189. Luong, T.Q.; Verma, P.K.; Mitra, R.K.; Havenith, M. Do hydration dynamics follow the structural perturbation during thermal denaturation of a protein: A terahertz absorption study. *Biophys. J.* **2011**, *101*, 925–933. [CrossRef] [PubMed]
190. George, D.K.; Chen, J.Y.; He, Y.; Knab, J.R.; Markelz, A.G. Functional-state dependence of picosecond protein dynamics. *J. Phys. Chem. B* **2021**, *125*, 11134–11140. [CrossRef]
191. Zhou, R.; Wang, C.; Wendao, X.; Xie, L. Biological applications of terahertz technology based on nanomaterials and nanostructures. *Nanoscale* **2019**, *11*, 3445–3457. [CrossRef] [PubMed]
192. Tang, Q.; Liang, M.; Yi, L.; Wong, P.K.; Wilmink, G.J.; Zhang, D.D.; Xin, H. Microfluidic devices for terahertz spectroscopy of live cells toward lab-on-a-chip applications. *Sensors* **2016**, *16*, 476. [CrossRef]

193. Zhao, X.; Zhang, M.; Wei, D.; Wang, Y.; Yan, S.; Liu, M.; Yang, X.; Yang, K.; Cui, H.; Fu, W. Label-free sensing of the binding state of MUC1 peptide and anti-MUC1 aptamer solution in fluidic chip by terahertz spectroscopy. *Biomed. Opt. Express* **2017**, *8*, 4427–4437. [CrossRef] [PubMed]
194. Cheng, R.; Xu, L.; Yu, X.; Zou, L.; Shen, Y.; Deng, X. High-sensitivity biosensor for identification of protein based on terahertz Fano resonance metasurfaces. *Opt. Commun.* **2020**, *473*, 125850. [CrossRef]
195. Amin, M.; Siddiqui, O.; Abutarboush, H.; Farhat, M.; Ramzan, R. A THz graphene metasurface for polarization selective virus sensing. *Carbon* **2021**, *176*, 580–591. [CrossRef] [PubMed]
196. Ahmadivand, A.; Gerislioglu, B.; Ramezzani, Z.; Kaushik, A.; Manickam, P.; Ghoreishi, A. Functionalized terahertz plasmonic metasensors: Femtomolar-level detection of SARS-CoV-2 spike proteins. *Biosens. Bioelectron.* **2021**, *177*, 112971. [CrossRef] [PubMed]
197. Xu, W.; Xie, L.; Zhu, J.; Xu, X.; Ye, Z.; Wang, C.; Ma, Y.; Ying, Y. Gold nanoparticle-based terahertz metamaterial sensors: Mechanisms and applications. *ACS Photonics* **2016**, *3*, 2308–2314. [CrossRef]
198. Adak, S.; Tripathi, L.N. Nanoantenna enhanced terahertz interaction of biomolecules. *Analyst* **2019**, *144*, 6172–6192. [CrossRef] [PubMed]
199. Zhang, Z.; Fan, F.; Shi, W.; Zhang, T.; Chang, S. Terahertz circular polarization sensing for protein denaturation based on a twisted dual-layer metasurface. *Biomed. Opt. Express* **2022**, *13*, 209–221. [CrossRef]
200. Meister, K.; Ebbinghaus, S.; Xu, Y.; Duman, J.G.; DeVries, A.; Gruebele, M.; Leitner, D.M.; Havenith, M. Long-range protein–water dynamics in hyperactive insect antifreeze proteins. *Proc. Natl. Acad. Sci. USA* **2013**, *110*, 1617–1622. [CrossRef]
201. Knab, J.; Chen, J.Y.; Markelz, A. Hydration dependence of conformational dielectric relaxation of lysozyme. *Biophys. J.* **2006**, *90*, 2576–2581. [CrossRef]
202. Heyden, M.; Havenith, M. Combining THz spectroscopy and MD simulations to study protein–hydration coupling. *Methods* **2010**, *52*, 74–83. [CrossRef]
203. Xu, J.; Plaxco, K.W.; Allen, S.J. Probing the collective vibrational dynamics of a protein in liquid water by terahertz absorption spectroscopy. *Protein Sci.* **2006**, *15*, 1175–1181. [CrossRef] [PubMed]
204. Pal, S.; Chattopadhyay, A. Hydration dynamics in biological membranes: Emerging application of terahertz spectroscopy. *J. Phys. Chem. Lett.* **2021**, *12*, 9697–9709. [CrossRef] [PubMed]
205. Wang, Y.; Wang, G.; Xu, D.; Jiang, B.; Ge, M.; Wu, L.; Yang, C.; Mu, N.; Wang, S.; Chang, C.; et al. Terahertz spectroscopic diagnosis of early blast-induced traumatic brain injury in rats. *Biomed. Opt. Express* **2020**, *11*, 4085–4098. [CrossRef] [PubMed]
206. Sun, Y.; Du, P.; Lu, X.; Xie, P.; Qian, Z.; Fan, S.; Zhu, Z. Quantitative characterization of bovine serum albumin thin-films using terahertz spectroscopy and machine learning methods. *Biomed. Opt. Express* **2018**, *9*, 2917–2929. [CrossRef] [PubMed]